Adsorptive removal of manganese(II) from the aqueous phase using iron oxide coated sand

R. Buamah, B. Petrusevski and J. C. Schippers

ABSTRACT

Iron oxide coated sand (IOCS) is a potential adsorbent for metallic ions, e.g. arsenic, lead, manganese etc., however the effect of process conditions and the mechanism of its adsorption of Mn(II) have not been thoroughly investigated. This study determined the capacity, rate, mechanisms involved and the effect of process conditions on the adsorption of Mn(II) onto IOCS using laboratory scale batch reactors with modeled water. Alkalinity and pH values of 8 and higher markedly affected the solubility of Mn(II) that is governed by manganese carbonate; solubility is very limited (1–2 mg/L or lower) even at low alkalinity (60 ppm).

The IOCS demonstrated an increasing adsorption capacity ('*K*' values: 4.73–147) of Mn(II) from pH values 6 to 8. For the initial short term, comparable adsorption capacity was found at pH 6 under both oxic and anoxic conditions. This indicates that no significant quantities of adsorbed Mn(II) were oxidized at pH 6 to form extra capacity within that period.

Kinetic studies using the linear driving force, Lagergren and potential driving second order kinetic (PDSOK) models revealed that the rate of manganese(II) adsorption onto aggregate IOCS declines after the initial phase likely due to the saturation of easily accessible adsorption capacities on grain surface and/or pH drop in the pores of the IOCS grains due to Mn(II) adsorption. The changing adsorption rate constants prevented the equilibrium concentration being predicted with the applied models.

Key words | adorption, iron oxide coated sand, manganese(II)

R. Buamah (corresponding author)
Water Supply and Environmental Sanitation,
Dept. of Civil Engineering,
Kwame Nkrumah University of Science and Technology, Kumasi,
Ghana
Tel.: +31(0)15 2151715 or +233(0)51 60235
Fax: +31(0)15 2122921 or +(0)51 60235
E-mail: *r.buamah@unesco-ihe.org*

B. Petrusevski
J. C. Schippers
UNESCO-The Institute for Water Education, Delft,
P.O. Box 3015, 2601, DA Delft,
The Netherlands

INTRODUCTION

Groundwater, by virtue of its generally good and constant quality, is popular as a drinking water resource. The presence of manganese in concentrations exceeding 0.1 mg/L may give rise to complaints about taste, staining of plumbing fixtures and turbidity (WHO 2004). In distribution systems manganese concentrations as low as 0.02 mg/L tend to form coatings on piping which later slough off as black precipitate. The present WHO guideline value of 0.4 mg/L recommended for manganese in drinking water is health-related (WHO 2004). Exposure to high manganese (> 0.5 mg/L) over the course of years has been associated with toxicity to the nervous system producing a syndrome that resembles Parkinsonism (Fact Sheet 2001).

Generally, aquifers possessing high levels of iron have appreciably high levels of manganese. Manganese concentrations are usually five to twenty times lower than iron concentrations in groundwater. Water treatment plants treating water with high iron and manganese frequently incorporate two filter stages; the first for the removal of mainly iron and some manganese and the second as a polishing step for iron and the removal of the main part of manganese. Sand filters used in the treatment of groundwater with high iron levels may normally end up having coated layers of iron oxides with manganese oxides embedded in the coating. Both the iron and manganese oxides in the coating of the media of such sand filters have

doi: 10.2166/aqua.2008.078

a high potential for the adsorption of heavy metal ions, e.g. As, Cr, etc. (Petrusevski *et al.* 2002). Iron oxide coated sand (IOCS) has given good indication of being a potential adsorbent for removal of Mn. The iron oxide present within the coating of the IOCS possibly enhances the autocatalysis of adsorbed Mn^{2+} and thereby forms manganese oxides (Junta & Hochella 1994). However, the mechanisms involved in the adsorption of metallic ions onto the IOCS and particularly the effects of oxic and anoxic conditions have not been well studied. This study seeks to investigate

- the effect of alkalinity on manganese solubility,
- the adsorption capacity of IOCS for manganese at different pH values,
- the effect of oxic and anoxic conditions on the manganese(II) adsorption,
- the kinetics and mechanism involved in the adsorption process,
- the effect of adsorbed Mn(II) on the rate of oxidation of manganese in the coating of the IOCS under oxic conditions.

THEORETICAL BACKGROUND

Solubility and oxidation states of manganese

Among the numerous oxidation states of manganese, the II, III and IV oxidation states are of greatest environmental importance. Mn(II) in aqueous solutions is stable at pH values below 9 because of its very low rate of oxidation. Therefore, in the range pH 6 to 9 of most natural waters, Mn(II) if present remains stable. Mn(II) oxidation results in the formation of Mn oxides which occur as coatings on soil and sediment particles and as discrete particles (Ehrlich 1996). Mn(II) exists in a variety of minerals such as birnessite ($Na_4Mn_{14}O_{27}{\cdot}9H_2O$), hollandite [$Ba(Mn^{4+}{\cdot}Mn^{2+})_8O_{16}$], rhodochrosite ($MnCO_3$), alabanite (MnS), reddingite [$Mn_3(PO_4)_2{\cdot}3H_2O$], etc. Mn(III) is thermodynamically unstable in aqueous solutions, being easily reduced to Mn(II) and can even undergo disproportionation reaction (e.g. Equation 5) in the absence of reducing agents (Cotton & Wilkinson 1967). Mn(III) does not occur in soluble form except in the presence of strong complexing agents such as humic acids or other organic acids (Kostka *et al.* 1995). Mn(III) and Mn(IV) primarily form insoluble oxides and oxyhydroxides. The solubility of manganese(IV) oxide (MnO_2) is very low within the pH range 3 to 10 (the solubility product: 10^{-41}, Stumm & Morgan 1996).

The concentration of dissolved Mn in groundwaters and surface waters is largely controlled by redox reactions between Mn(II) and Mn(III,IV) and governed by pH. Mn(II) oxidation in such natural systems is thermodynamically favourable but often proceeds at very slow rates. According to Murray *et al.* (1985), under more extreme conditions (pH $>$ 8.5, oxygen partial pressure of 1 atm or $[Mn_{Total}] > 25$ mg/L) Mn(II) homogeneously oxidizes within a few weeks to months. The Mn(II) oxidation is autocatalytic with the Mn-(oxyhydr)oxide products adsorbing Mn(II) and catalysing its oxidation (Stumm & Morgan 1996). The Mn(II) oxidation may also be catalysed by a variety of other surfaces including Fe oxides and silicates (Junta & Hochella 1994). Mn(II) oxidation proceeds via a number of reactions yielding various oxidation states and mineral forms. Mn(II) can be oxidized directly to Mn(IV) or to mixed Mn(II) and Mn(III) oxides and oxyhydroxides or to Mn_3O_4 (composed of $Mn_2O_3{\cdot}MnO$). These mixed oxides may undergo protonation or disproportionation reactions (the rate determining step) to form Mn(IV) oxides and manganates, i.e. the '6-valent manganese' (Murray *et al.* 1985).

$$Mn^{2+} + 1/2O_2 + H_2O \rightarrow MnO_2 + 2H^+ \quad (1)$$

$$Mn^{2+} + 1/4O_2 + 3/2H_2O \rightarrow MnOOH + 2H^+ \quad (2)$$

$$3Mn^{2+} + 1/2O_2 + 3H_2O \rightarrow Mn_3O_4 + 6H^+ \quad (3)$$

$$Mn_3O_4 + 2H^+ \rightarrow 2MnOOH + Mn^{2+} \quad (4)$$

$$Mn_3O_4 + 4H^+ \rightarrow MnO_2 + 2Mn^{2+} + 2H_2O \quad (5)$$

The adsorption phenomenon

The adsorption phenomenon involves the separation of a substance from one phase accompanied by its concentration on the surface of another. The adsorbing phase is the adsorbent and the material concentrated is the adsorbate. The character of the quantitative equilibrium distribution

between the phases which affects the adsorption is influenced by a variety of factors. These factors relate to the properties of the adsorbate, the adsorbent and the system in which the adsorption occurs (Slejko 1985).

Adsorption on a surface or interface is the result of binding forces between the individual atoms, ions or molecules of the adsorbate and the surface; these forces have their origin in electromagnetic interactions (Van Vliet & Weber Jr. 1981). The interactions between adsorbate and adsorbent consist of molecular forces embracing permanent dipole, induced dipole and quadruple electrostatic effects. These forces may be classified into short range forces (i.e. the chemical forces) and long range forces (i.e. the coulombic forces). The short range forces may give rise to covalent or hydrophobic bonds or hydrogen bonding or steric effect. The long range forces give rise to electrostatic attraction (Yang 1999). Based upon these adhesive forces four principal types of adsorption have been identified: namely, ion exchange, chemical adsorption, physical adsorption and specific adsorption (Yang 1999).

Ion exchange

Ion exchange involves short-range forces and normally occurs within materials with porous lattice containing fixed charges. In ion exchange, the electrostatic attachment of ionic species to sites of opposite charge at the surface of an adsorbent occurs with a subsequent displacement of these species by other ionic adsorbates of greater electrostatic affinity. This substitution generally results in the emergence of a net charge on the surface of the adsorbent. Consequently in aqueous solutions the electrostatic attraction brings dissolved ions of opposite charge to the adsorbent to balance the charge (Deutsch 1997). Ion exchange may involve either a cation exchange or an anion exchange and in both cases pH changes play a vital role in the exchange capacity.

Chemical adsorption

Chemical adsorption involves a reaction between an adsorbate and adsorbent resulting in a change in the chemical form of the adsorbate. Sharing of electrons between the adsorbent and the adsorbate occurs at the adsorptive site of the adsorbent yielding process irreversibility. Adsorption onto hydrous metal oxides surface, e.g. hydrous iron oxide or manganese oxide, is predominantly, chemical adsorption.

According to Davis & Leckie (1978) the adsorption on hydrous metal oxide involves surface ionization and surface complexation of metal ions with the hydrous metal oxide. In aqueous systems the surface of the metal oxide gets covered with hydroxyl groups. An acid–base equilibrium involving the hydroxylated oxide surface is established as follows:

$$\equiv S-OH + H^+ \leftrightarrow \equiv S-OH_2^+ \quad (6)$$

$$\equiv S-OH \leftrightarrow \equiv S-O^- + H^+ \quad (7)$$

where $\equiv S-OH_2^+$, $\equiv S-OH$ and $\equiv S-O^-$ represent positively, neutral and negatively charged surface hydroxyl respectively. From these representations the point of zero charge (P_{zc}) can be depicted as '$\equiv S-OH$'. The P_{zc} is the pH of the solution in chemical equilibrium with the surface in its neutralized state through adsorption of H^+ and/or OH^- ions (Casamassima & Darque-certti 1993). Mn oxides have a very negative charge at pH values higher than their P_{zc} and their cation adsorption capacity therefore generally increases with increasing pH (Liu *et al.* 2004). At pH values below their P_{zc} the net surface charge is positive and anion adsorption is favoured.

In the surface complexation, initially a bond is formed between the metal ion to be adsorbed and the surface oxygen atom of the hydrous metal oxide resulting in the release of protons and a drop in pH:

$$\equiv S-OH + M^{2+} \leftrightarrow \equiv S-OM^+ + H^+ \quad (8)$$

where M^{2+} is a divalent cation.

In aqueous solution with low pH values, the surface is more positively charged because of the additional complexed hydrogen ions producing $\equiv S-OMOH_2^+$ and loss of OH^-.

$$\equiv S-OH + M^{2+} + H_2O \leftrightarrow \equiv S-OMOH_2^+ + H^+/OH^- \quad (9)$$

At a higher pH condition the surface is predominantly negatively charged due to the loss of H^+ from the surface

and subsequently the surface becomes more attractive to cations.

$$\equiv S-OH + M^{2+} + H_2O \leftrightarrow \equiv S-OMO^- + 3H^+ \quad (10)$$

Physical adsorption

Physical adsorption generally results from the action of van der Waals forces that hold the adsorbate molecule to the atoms on the adsorbent surface. The adsorbed molecule is not affixed to a specific site but free to undergo translational movements.

Specific adsorption

Specific adsorption involves attachment of adsorbate molecules at functional groups on adsorbent surfaces. In these interactions the adsorbate does not undergo any transformation. Specific adsorption exhibits a range of binding energies common to both chemical and physical adsorption.

Freundlich's adsorption isotherm

Freundlich's adsorption isotherm is commonly used to describe the adsorption capactity of coated materials; however, the Langmuir isotherm can be used as well. In this article, Freundlich's isotherm is used. Expressed mathematically,

$$q = KC_s^{1/n} \quad (11)$$

where q, amount of adsorbate adsorbed per unit mass or surface area of the adsorbent (g/g or g/m^2); C_s, equilibrium concentration of the adsorbate (g/m^3); K and n are isotherm constants. K[(mg/g) × (mg/L)^n] gives an indication of the adsorption capacity while n (a constant with no dimension) is a measure of the adsorption intensity and also reflects the steepness of the curve whether plotted on an arithmetic or logarithmic scale (Faust & Aly 1998).

Adsorption kinetic models

Several kinetic models are available for studying adsorption kinetics. In this article three models, namely the linear driving force model (LDF), the Lagergren model and the potential driving second order kinetic model (PDSOK) are applied to investigate the rate of adsorption of Mn(II) onto IOCS in batch experiments.

The linear driving force model

The linear driving force model is an approach which employs an overall kinetic rate constant (covering both internal and external mass transfer coefficients) in defining the adsorption rate equation. According to the LDF equation, the rate of adsorption of an adsorbate (i.e. Mn(II)) by an adsorbent (in this case IOCS) is linearly proportional to the driving force. The driving force is defined as the difference between the surface concentration and the average adsorbed phase concentration (Tien 1994). Mathematically,

$$\frac{dq}{dt} = k_1(q_s - q) \quad (12)$$

where q, the solid phase manganese(II) concentration (kg/kg); q_s, the solid phase manganese(II) concentration in equilibrium with c_s (kg/kg); k_1, the LDF kinetic rate constant (s^{-1}); t, time (s).

Using Freundlich's isotherm equation and mass balance, the above equation could be re-written expressing the q in terms of the initial liquid phase manganese(II) concentration

$$c = (c_0 - c_s)e^{-k_1 t} + c_s \quad (13)$$

In natural logarithimic form

$$\ln[(c - c_s)/(c_0 - c_s)] = -k_1 t \quad (14)$$

where c, the liquid phase manganese(II) concentration (kg/m^3) at time t; c_0, the initial liquid phase manganese(II) concentration (kg/m^3) at time t_0; c_s, the liquid phase manganese(II) concentration near the particle surface (kg/m^3); k_1, the LDF rate constant, can be obtained from the kinetic data of a batch adsorption experiment.

The Lagergren model

To determine the order of the adsorption, the Lagergren's equation is applied (El Zawahry & Kamel 2004).

$$\log(q_s - q) = \log q_s - tk_2/2.303 \quad \text{(Lagergren's equation)} \quad (15)$$

where q, the amount of Mn^{2+} (g/L) adsorbed at time t; q_s, the amount of Mn^{2+} adsorbed (g/L) at equilibrium; k_2, the rate constant for the adsorption process. k_2 can be determined from the slope of the linear plot of $\log(q_s - q)$ versus t. Linearity of plot will be an indication that the reaction taking place is of the first order.

The potential driving second order kinetic model

The PDSOK assumes that the most important factors influencing the adsorption process are the chemical potentials of both the adsorbent surface and the solution. The chemical potentials are, in turn influenced by the contact time, temperature, pH, adsorbent concentration, nature of the solute and its concentration. The PDSOK model could be used to investigate among others, the order of the reaction (Liu *et al.* 2004). For the PDSOK model, the rate differential equation for the adsorption process is expressed as follows:

$$\frac{dc}{dt} = -k_3(s_s - s)(c - c_s) \tag{16}$$

where c_s, Mn^{2+} concentration (mol/L) in the liquid phase at equilibrium; c, Mn^{2+} concentration (mol/L) in the liquid phase at time t; s, the number of active sites on the adsorbent occupied (mol/g) at time t; s_s, the number of active sites on the adsorbent occupied (mol/g) at equilibrium; a, the adsorbent dosage (g/L); k_3, the rate constant.

This implies that

$$s = (c_0 - c)/a \tag{17}$$

where c_0, Mn^{2+} concentration (mol/L) in the liquid phase at time t_0.

$$s_s = (c_0 - c_s)/a \tag{18}$$

Substituting for s and s_s in Equation (16) and rearranging gives

$$-dc/(c_s - c)^2 = k_3 dt/a \tag{19}$$

Integrating with boundary conditions $t = 0$ and $t = t$ and c_0 to c yields

$$1/[(c_0 - c_s) - (c_0 - c)] = 1/(c_0 - c_s) + k_3 t/a \tag{20}$$

Rearranging Equation (20) gives rise to the following:

$$t/(c_0 - c) = t/(c_0 - c_s) + a/k_3(c_0 - c_s)^2 \tag{21}$$

The rate constant k_3 and equilibrium concentration c_s can be determined experimentally by plotting $t/(c_0 - c)$ against t.

MATERIALS AND METHODS

Materials for batch studies

In this study, IOCS collected from the Noord Bargeres groundwater treatment plant in The Netherlands, was used as the adsorbent. The main function of these rapid sand filters at the plant is the removal of iron, manganese and some ammonium. The water quality of the groundwater treated at the plant is given in Table 1 (Sharma 2002).

From the composition analysis on the IOCS, it was found that 509 mg iron and 24.5 mg manganese were present per gram of IOCS. Both pulverised form (particle size: < 65 μm) and aggregate form (particle size: 2.00–3.15 mm) of the IOCS were used in the study. The pulverised IOCS was used in order to provide a larger surface area which would increase the rate of adsorption. The pulverised IOCS was used in most experiments since the adsorption process on aggregate IOCS was very slow and predictions of the ultimate adsorption capacity by making use of kinetic models were not successful. At most water treatments plants, the sand filter media normally remains in use for several years before replacement. During the period, the adsorbed ions penetrate and diffuse into the pores within the coating of the sand grains thereby gradually increasing the adsorption capacity of the coated sand grain with time. The use of aggregate media for batch experiments may underestimate the adsorption potential of the media. With the pulverised

Table 1 | Composition of groundwater treated at the treatment plant in Noord Bargeres

pH	Fe (mg/L)	Mn (mg/L)	Ca^{2+} (mg/L)	Mg^{2+} (mg/L)	Cl^- (mg/L)	SO_4^{2-} (mg/L)	HCO_3^- (mg/L)	NH_4^+ (mg/L)	DOC (mg/L)
6.9	13.3	0.49	50	6.5	36	57	128	0.2	2.0

media, much of the less accessible pores are opened up and the adsorption capacities determined from the experiment would be close to the ultimate adsorption capacity of the media. Over-estimation of the capacity may not be excluded in this case.

To ascertain the role of sand material in the adsorption experiments, de-coated IOCS was tested for its manganese adsorption capacity. For this purpose 1 g of pulverised IOCS was treated in 6 N HCl solution over 24 hours to dissolve the coating completely, washed with de-mineralised water and dried.

Batch experiments

Batch experiments were done under oxic and anoxic conditions with model water. Most groundwaters have Mn(II) concentrations of up to 2 mg/L, however on rare occasions Mn(II) concentrations could go up to about 10 mg/L. A stock solution of concentration 1000 mg Mn(II)/L was prepared using analytical-grade $MnSO_4{\cdot}H_2O$ and acidified with concentrated HCl (32% assay) to a pH < 2. The maximum Mn(II) concentrations at the various pH for which interference of possible $MnCO_3$ precipitation is avoided, were calculated using solubility product equations (Stumm & Morgan 1996) and the Phreeqc software programmes (Parkhurst & Appelo 1999). Experiments were performed with initial Mn(II) concentrations of up to 10 mg/L to enable a high accuracy, prevent manganese carbonate precipitation and simulate the range of manganese levels in groundwaters. To ensure a stable pH during experiments, $NaHCO_3$ was added to the model water.

For the oxic experiments acid-cleansed 500 mL plastic bottles fitted with tubes for periodic sampling were filled with de-mineralized water dosed with the appropriate amount of $NaHCO_3$ (Table 2) and their pH subsequently adjusted with 6 N HCl or 1 N solutions to the required level. After thorough mixing of the prepared model water, they were dosed with Mn(II) and 4 g of pulverised, aggregate IOCS or de-coated IOCS were added. Bottles were kept at 20 ± 1°C and placed on a shaker. Blank tests were carried out without the addition of (de-coated) IOCS.

Experiments under anoxic conditions were in 1.5 L glass reactors with model water (Table 2) and a dosage of 8 g IOCS/L. Nitrogen gas was infused into the reactor to attain and maintain anaerobic conditions. Carbon dioxide was introduced for pH adjustment. Mixing was ensured by the gas infusions and continuous stirring. Periodic sampling was done at regular time intervals to determine the rate of adsorption and equilibrium conditions. Equilibrium was considered to have been reached when the difference in manganese concentration of two consecutive samples taken over a period of 10 hours was ≤ 0.02 mg/L.

All experiments were run in duplicate and samples filtered through a 0.45 μm membrane filter using a polypropylene syringe filter. Manganese analysis was done using Perkin Elmer 3110 spectrometer in accordance with the Dutch Standard Method NEN 6457. The method used has a detection level of 0.02 mg Mn(II)/L. The LDF, Lagergren's and PDSOK models were tested with the data from the batch experiments performed at pH 6 under anoxic conditions.

RESULTS AND DISCUSSIONS

The effect of pH and hydrogen carbonate concentration on the solubility of manganese(II)

The calculated data obtained from the solubility product equations and the Phreeqc software programmes were used

Table 2 | Experimental conditions for the batch experiments

	Oxic experiment				Anoxic experiment			
	pH 5	pH 6	pH 7	pH 8	pH 5	pH 6	pH 7	pH 8
$[NaHCO_3]$ (mg/L)	1000	1000	84	42	1000	1000	84	84***
$[Mn^{2+}]$ (mg/L)	2	2	2	2	0.1–10	0.1–10	0.1–8	0.1–1.0

*** In cases where anoxic experiments performed at pH 8 required initial manganese concentration of 2 mg/L, the sodium hydrogen carbonate added was 42 mg/L.

to develop Figure 1 which shows the solubility of Mn(II) as a function of pH and hydrogen carbonate concentration. From Figure 1 it follows that at pH 7 and 8 and hydrogen carbonate concentration of 61 mg/L, manganese concentrations (in the aqueous solution) should be kept below 10 mg/L and 1 mg/L respectively. The blank tests performed indicated that upon exceeding approximately 1 mg Mn(II)/L concentration in the aqueous solution at pH 8 with 61 mg HCO_3^-/L, precipitation just begins to occur (Figure 2). At pH 5 and 6 solubility of manganese carbonate is sufficiently high to avoid precipitation even at the hydrogen carbonate concentration of 1000 mg/L. Groundwater frequently demonstrates high HCO_3^- concentrations of up to 450 mg HCO_3^-/L. These values, together with pH values above 7 might explain why manganese concentrations in groundwaters do not usually exceed 2 mg/L. In groundwater treatment, the standard practical process of aeration prior to filtration normally results in an increase in pH as carbon dioxide is stripped off. With this practice, the precipitation of manganese carbonate might play a beneficial role when the hydrogen carbonate and pH are at relatively high levels.

Adsorption isotherms

Initially the anoxic conditions were chosen to eliminate the potential catalytic oxidation of adsorbed Mn(II). Batch adsorption experiments conducted under the anoxic conditions always proceeded to an equilibrium position after a certain period.

The adsorption data fitted reasonably the Freundlich isotherm (Figure 3). Equilibrium for the pulverized IOCS experiments was normally attained from 10 to 48 hours for the various pH values. Figure 3 shows that manganese can be removed by adsorption in practice.

The *K* values on Table 3 show pronounced increase in the manganese adsorption capacity of the pulverized IOCS with increasing pH. This increase in the adsorption capacity together with expected high rate of oxidation at higher pHs (Stumm & Morgan 1996) is in consonance with what happens in practice.

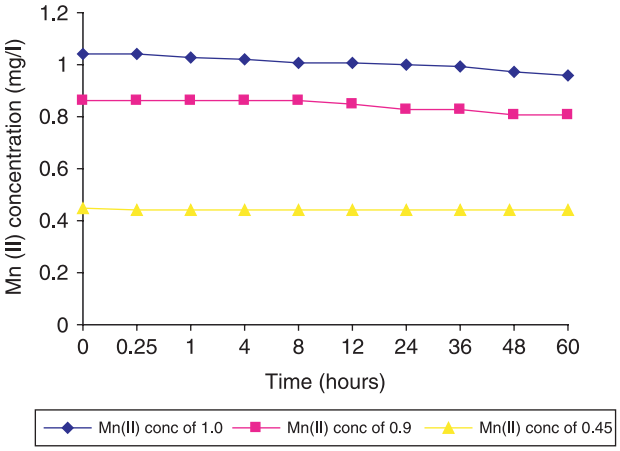

Figure 2 | Mn(II) solubility at pH 8, 61 mg HCO_3^-/L and anoxic conditions (blank test).

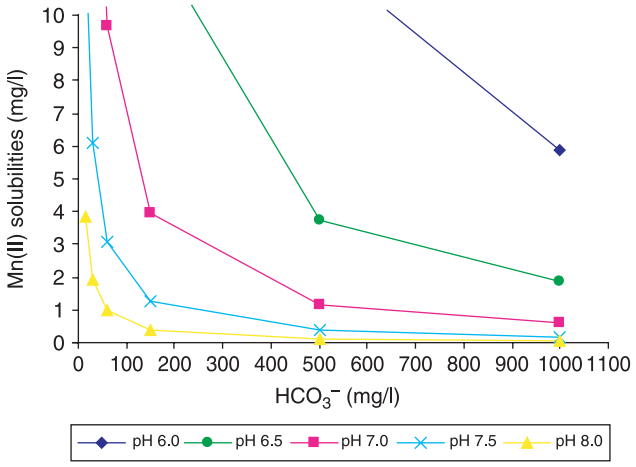

Figure 1 | Effect of alkalinity on manganese(II) solubility at various pH values (dots are calculated data).

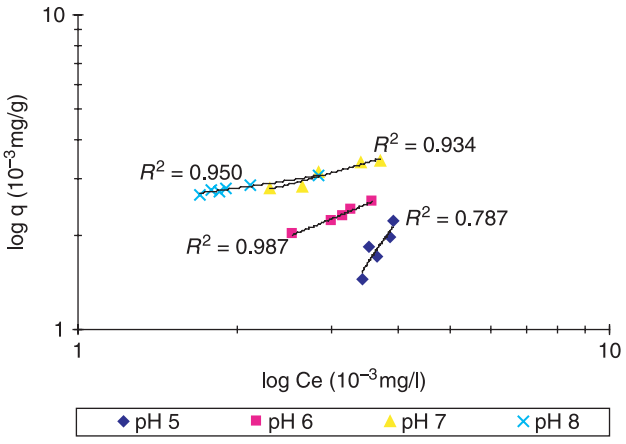

Figure 3 | Anoxic manganese adsorption isotherms of pulverized IOCS. Test conducted with 1000 mg $NaHCO_3$/L for pH 5 and 6 and 84 mg $NaHCO_3$/L for pH 7 and 8.

Table 3 | The Freundlich's isotherm constants obtained at the various pH values

	pH 5	pH 6	pH 7	pH 8
K	0.0024	4.73	45.84	147
n	0.83	1.91	2.02	3.08

Unit of K: $[10^{-3}\,mg/g \times (10^{-3}\,mg/L)^n]$.

Adsorption equilibrium studies

Comparative performance of pulverised, aggregate and de-coated IOCS

Under anoxic conditions at pH 6, it was observed that pulverised IOCS had equilibrium state established after 10–12 hours, having achieved about 80% manganese removal at an initial concentration of 2 mg Mn(II)/L (Figure 4). Equilibrium for the IOCS (aggregate) was established after 80 hours, having removed about 70% of manganese. Pulverised IOCS consequently demonstrated a higher adsorption capacity than aggregate IOCS. This difference in capacity is attributed to the opening and shortening of pores during grinding. In the aggregates a part of the pores is most likely not accessible.

The effect of oxic and anoxic conditions on the manganese adsorption

The trends of manganese adsorption unto the aggregate media under oxic and anoxic conditions were found to be similar within the first 24 hours of operation (Figure 5a). This indicates that no substantial quantities of adsorbed Mn(II) were oxidized under the oxic conditions at pH 6 to form extra capacity within that experimental period.

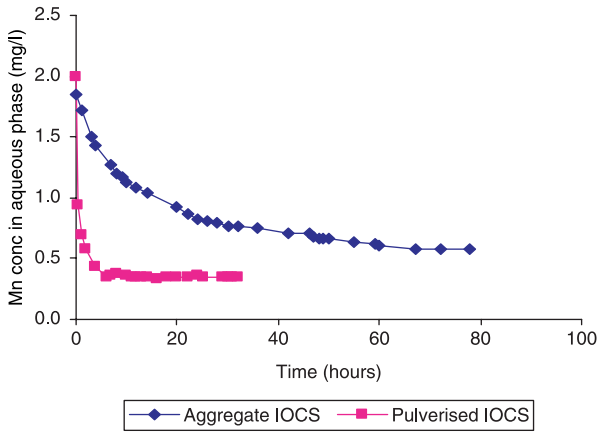

Figure 4 | Performance of aggregate and pulverised IOCS in manganese adsorption under anoxic conditions at pH 6, 1000 mg $NaHCO_3$/L, initial Mn(II) concentration of 2 mg/L and 8 g IOCS/L.

Under both oxic and anoxic conditions in the reactor, the adsorption process was faster than in the shaker (under oxic condition). This indicates that the reactor, using a mechanical stirrer, created a more effective (external) mass transfer (Figure 5a).

In Figure 5b, the de-coated IOCS demonstrated a very low manganese adsorption capacity thereby confirming the fact that the adsorption process was predominantly due to the adsorptive activity of the mineral coating of the media (Figure 5b). A blank test resulted in a negligible reduction of manganese concentration.

Effect of pH on manganese adsorption under oxic conditions

Figure 6 demonstrates that adsorption under oxic conditions on pulverised IOCS takes a very long time (250 hours). This effect might be attributed to a catalytic effect of adsorbed Mn(II) that has been oxidised to MnO_2 or Mn_3O_4. The latter oxides might have acted as a catalyst and created new adsorption sites, however the amount of adsorbed manganese is much lower than the amount present within the coating material. Owing to the lower manganese levels observed at the latter stages (i.e. >100 hours) for the higher pHs 7 and 8, the expected catalytic effect due to the oxidation of adsorbed manganese could not be ascertained (Figure 6). More likely is the possibility of movement of the adsorption front within the IOCS particles entering pores which are narrower and consequently resulting in a slow but continuing adsorption. The increasing adsorption potential of the media with increasing pH is a trend which is in agreement with the findings of most researchers (Post 1999).

The P_{zc} of the manganese oxides in the IOCS may be less than pH 5, therefore as pH of the aqueous solution increases from 5 to 8, the density of negative charges on the IOCS particles correspondingly increases. This leads to a greater electrostatic attraction for cations, thus increasing the adsorption of manganese. Moreover, the oxidation of adsorbed Mn(II) could also be enhanced with increasing pH.

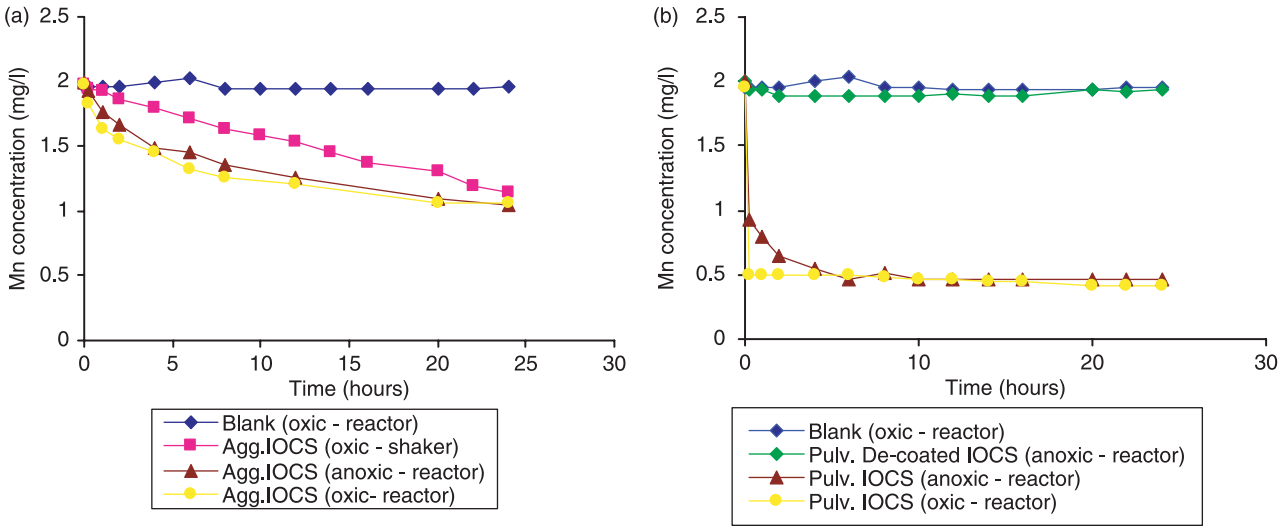

Figure 5 | Comparative performance of (a) aggregate (b) pulverised IOCS in Mn(II) adsorption under oxic and anoxic conditions using 8 g IOCS/L in both reactor and shaker experiments at pH 6 with 1000 mg $NaHCO_3$/L and initial Mn(II) concentration of 4 mg/L.

The oxic experiments showed that the manganese removal proceeded with a drop in pH; indicating a release of protons. This evidence signifies that the manganese removal presumably involves the chemical adsorption and/or ion exchange as the predominant removal mechanism.

Adsorption kinetic study

Some of the kinetic data obtained from the anoxic experiments with the reactor were tested by fitting to the LDF, Lagergren and PDSOK models (Figures 7 and 8). For the LDF model (Figure 7a) it was found that the slope for the aggregate IOCS was initially steep, subsequently flattened and finally increased again.

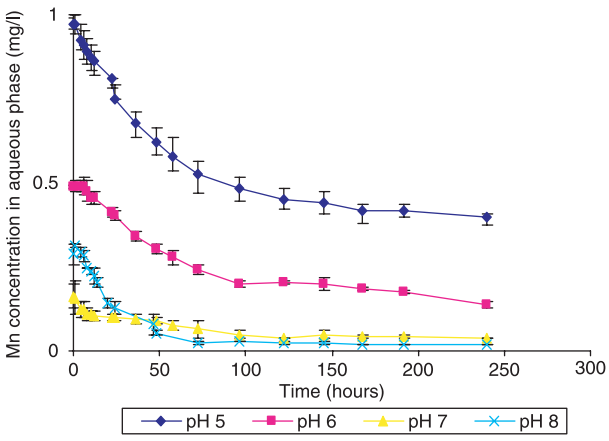

Figure 6 | Effect of pH on manganese adsorption onto pulverised IOCS under oxic conditions. Test conducted with 1000 mg $NaHCO_3$/L, for pH 5 and 6 and 42 mg $NaHCO_3$/L for pH 7 and 8; initial Mn(II) concentration of 2 mg/L and 8 g IOCS/L.

The pulverised IOCS demonstrated similar behaviour; however, the flattening trend was less distinct. This phenomenon of the pulverised IOCS might be attributed to the faster exhaustion of the adsorption sites which are easily accessible and their pores possibly shorter in length. Another explanation could be the effect of pH on the adsorption of Mn(II). The adsorption results in release of H^+ which leads to a local drop in pH within the pores. According to Figures 3 and 6, the adsorption capacity drops substantially at lower pH values. Finally, the slope increases, which is the result of the fact that the concentration c approaches the equilibrium concentration c_s.

According to the re-arranged Equation (14)

$$\ln(c_0 - c_s)/(c - c_s) = k_1 t \tag{22}$$

k_1 tends to become infinite as soon as c equals c_s.

The Lagergren and PDSOK models demonstrated the same behaviour as the LDF model; demonstrating an initially steep slope, subsequently flattening and finally increasing again. The PDSOK plots however, exhibited a much higher linearity with a very constant slope for the pulverised IOCS as shown in Figure 8. In addition, the

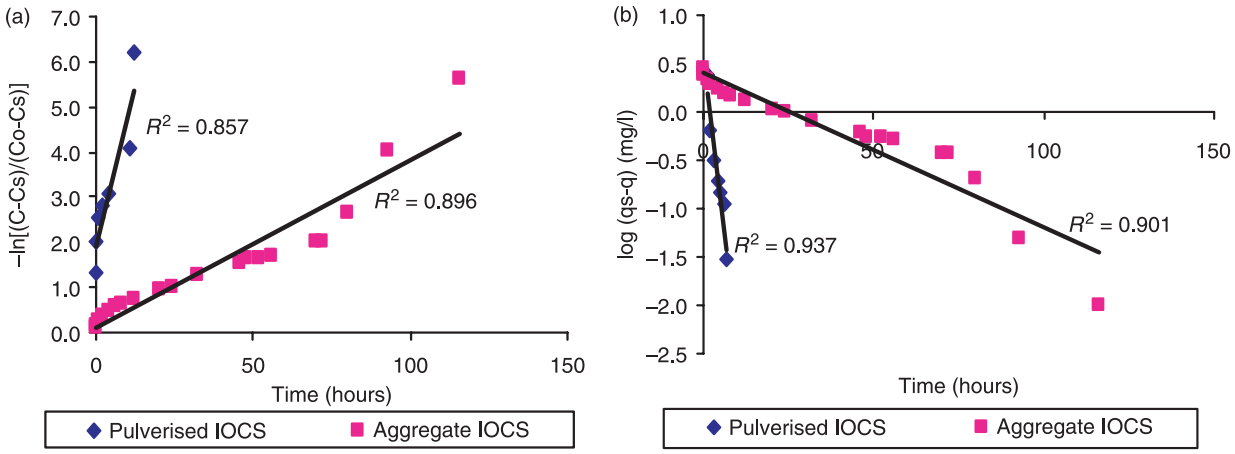

Figure 7 | Kinetic models: (a) linear driving force model (LDF); (b) Lagergren's model. Test conducted at pH 6 with 1000 mg $NaHCO_3$/L, initial Mn(II) concentration of 4 mg/L and 8 g IOCS/L.

flattening effect is less defined for the aggregate in the PDSOK plots.

The observed linearity in the later part of the curve for the aggregate in the PDSOK plot is linked to Equation (21), which shows that the slope of the curve will gradually become a constant namely, $1/(c_0 - c_s)$. The changing slopes prevent using the models for predicting the remaining concentration as a function of time since the k-value varies in time. Consequently, the predicted value c_s will vary in time.

This conclusion excludes the possibility of shortening adsorption isotherm measurements on aggregate IOCS. Measurements on pulverised IOCS reach equilibrium much faster: however, the observed adsorption capacity is likely somewhat larger than the aggregate IOCS's capacity.

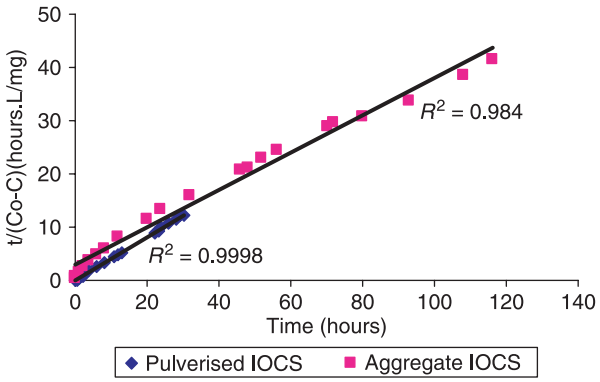

Figure 8 | Potential driving second order kinetic model (PDSOK). Test conducted at pH 6 with 1000 mg $NaHCO_3$/L, initial Mn(II) concentration of 4 mg/L and 8 g IOCS/L.

CONCLUSION

- Alkalinity and pH have a marked effect on solubility of Mn(II). This solubility is governed by the formation of manganese carbonate. Manganese hydroxide has a much higher solubility. At pH values of 8 and higher, calculated solubility of Mn(II) is very limited (1–2 mg/L or lower) even at low alkalinity (60 ppm).
- IOCS demonstrated a substantial adsorption capacity for manganese(II) under anoxic and oxic conditions. Adsorption data fit reasonably well the Freundlich isotherm model. Adsorption capacities ('K' values increase from 0.0024 to 147) increase from pH 5 to 8 and, remarkably, n the range of pH 7 to 8.
- The rate of adsorption of Mn(II) on IOCS at pH 6 is identical under oxic and anoxic conditions. Therefore there is no indication that under oxic conditions at pH 6, adsorbed Mn(II) is oxidised and additional adsorption capacity formed.
- Plots of the kinetic models, i.e. linear driving force, Lagergren and potential driving second order kinetic models show a reasonable linearity. However, for aggregate IOCS, the initial slopes decreased with progressing adsorption. This phenomenon might be attributed to the presence of easily accessible and less accessible adsorption sites (e.g. in narrow pores) and/or decreasing pH in the pores as a result of Mn(II) adsorption on IOCS.
- Predicting the equilibrium concentration making use of three kinetic models turned out to be not a feasible

option due to changing adsorption rate constants in the course of the adsorption process.

Further studies on the manganese adsorption mechanisms and the oxidation kinetics of the adsorbed manganese are on going.

REFERENCES

Casamassima, M. & Darque-Ceretti, E. 1993 Correlation between Lewis donor/acceptor properties determined by XPS and Bronsted acid/base properties determined by rest-potential measurements, for aluminium and silicon oxides. *J. Mater. Sci.* **28**, 3997–4002.

Cotton, F. A. & Wilkinson, G. 1967 The transition elements. *Advanced Inorganic Chemistry–A Comprehensive Text*, 2nd edition. Interscience Publishers–A division of John Wiley & Sons, New York, pp. 837–838.

Davis, J. A. & Leckie, J. O. 1978 Surface ionization and complexation at the oxide/water interface: surface properties of amorphous iron oxyhydroxide and adsorption of metal ions. *J. Colloid Interface Sci.* **67**(1), 90–107.

Deutsch, W. J. 1997 Water/rock interactions. *Groundwater Geochemistry–Fundamentals and Applications to Contamination*. Lewis Publishers–CRC Press LLC, Boca Raton, Florida–USA, pp. 47–60.

Ehrlich, H. L. 1996 *Geomicrobiology*. Marcel Dekker, New York, USA.

El Zawahry, M. M. & Kamel, M. M. 2004 Removal of azo and anthraquinone dyes from aqueous solutions by Eichhornia Crassipes. *Wat. Res.* **38**, 2967–2972.

Fact Sheet July 2001 *What You Need to Know About Manganese in Drinking Water*. http: www.dph.state.ct.us/publications/BCH/EEOH/manganese Division of Environmental Epidemiology and Occupational Health. Hartford, CT 06134–0308.

Faust, S. D. & Aly, O. M. 1998 *Chemistry of Water Treatment*, 2nd edition. Lewis Publishers–CRC Press LLC, Boca Raton, pp. 145–146, Ann Arbor Science book.

Junta, J. L. & Hochella, Jr. M. F. 1994 Manganese (II) oxidation at mineral surfaces: a microscopic and spectroscopic study. *Geochim Cosmochim Acta* **58**, 4985–4999.

Kostka, J. E., Luther, G. W. III & Nealson, K. H. 1995 Chemical and biological reduction of Mn (III) pyrophosphate complexes-potential importance of dissolved Mn (III) as an environmental oxidant. *Geochim Cosmochim Acta* **59**, 885–894.

Liu, D., Sansalone, J. J. & Cartledge, F. K. 2004 Adsorption characteristics of oxide coated buoyant media ($\ell s < 1.0$) for storm water treatment I: Batch Equilibra and Kinetic models. *J. Environ. Eng.* **130**(4), 383–390.

Murray, J. W., Dillard, J. G., Giovanoli, R., Moers, H. & Stumm, W. 1985 Oxidation of Mn (II): initial mineralogy, oxidation state and aging. *Geochim Cosmochim Acta* **49**, 463–470.

Parkhurst, D. L. & Appelo, C. A. J. 1999 *User's Guide to Phreeqc (Version 2) – A Computer Program for Speciation, Batch-Reaction, One-dimensional Transport and Inverse Geochemical Calculations*. U.S. Geological Survey Water-Resources Investigations Report 99-4259.

Petrusevski, B., Boere, J., Shahidullah, S. M., Sharma, S. K. & Schippers, J. C. 2002 Adsorbent based point-of-use system for arsenic removal in rural areas. *J. Water Supply Res. Technol.* **51**, 135–144.

Post, J. E. 1999 Manganese oxide minerals: Crystal structures and economic and environmental significance. Colloquim paper. *Proc. Natl. Sci.* **96**, 3447–3454.

Sharma, S. K. 2002 *Adsorptive Iron Removal from Groundwater*. PhD Thesis. Unesco-IHE, Institute for Water Education and Wageningen University. Swets and Zeitlinger B.V., Lisse.

Slejko F. L. 1985 Adsorption Technology–A step-by-step Approach to Process Evaluation and Application. In: *Chemical Industries Series Vol. 19*. Slejko, F. L. (ed). Tall Oaks Publishing Inc. Voorhees, New Jersey, pp. 18–30.

Stumm, W. & Morgan, J. J. 1996 *Aquatic Chemistry: Chemical equilibria and Rates in Natural Waters*, 3rd edition. Wiley, New York, USA, pp. 684–685.

Tien, C. 1994 Adsorbate transport: Its adsorption and rates. In: *Adsorption calculations and Modeling* (Brenner, H. Ed). Butterworth-Heinemann, Boston, pp. 81–82.

Van Vliet, B. M. & Weber, W. J. Jr. 1981 Comparative performance of synthetic adsorbents and activated carbon for specific compound removal from wastewaters. *J. Water Poll. Control Fed.* **53**(11), 1585–1598.

WHO 2004 *Guidelines for Drinking-Water Quality*, 3rd edition (Vol. 1). WHO, Geneva, Recommendations.

Yang, R. T. 1999 *Gas Separation by Adsorption Processes.–Series on Chemical Engineering*, (Vol. 1.). Publishers–Imperial College Press, London, UK.

First received 4 October 2006; accepted in revised form 25 June 2007